RADAR
Research Archive and Digital Asset Repository

OXFORD BROOKES UNIVERSITY

La Rocca, A, Bonatesta, F, May, M and Campanella, F

Characterisation of soot in oil from a gasoline direct injection engine using transmission electron microscopy.

La Rocca, A, Bonatesta, F, May, M and Campanella, F (2015) Characterisation of soot in oil from a gasoline direct injection engine using transmission electron microscopy. *Tribology International*, 86. pp. 77-84.

doi: 10.1016/j.triboint.2015.01.025

This version is available: https://radar.brookes.ac.uk/radar/items/454829b3-820b-4739-8476-a1b8c33a45df/1/

Available on RADAR: September 2016
Copyright © and Moral Rights are retained by the author(s) and/ or other copyright owners. A copy can be downloaded for personal non-commercial research or study, without prior permission or charge. This item cannot be reproduced or quoted extensively from without first obtaining permission in writing from the copyright holder(s). The content must not be changed in any way or sold commercially in any format or medium without the formal permission of the copyright holders.

This document is the published version of the journal article.

WWW.BROOKES.AC.UK/GO/RADAR

Tribology International 86 (2015) 77–84

Contents lists available at ScienceDirect

Tribology International

journal homepage: www.elsevier.com/locate/triboint

# Characterisation of soot in oil from a gasoline direct injection engine using Transmission Electron Microscopy

A. La Rocca [a,*], F. Bonatesta [b], M.W. Fay [a], F. Campanella [a]

[a] Department of Mechanical Materials and Manufacturing Engineering, University Park, Nottingham NG7 2RD, UK
[b] Department of Mechanical Engineering and Mathematical Science, Oxford Brookes University, Wheatley Campus, Oxford OX33 1HX, UK

ARTICLE INFO

*Article history:*
Received 2 November 2014
Received in revised form
19 January 2015
Accepted 31 January 2015
Available online 9 February 2015

*Keywords:*
Gasoline soot
Lubrication oil
Nanoparticles
Transmission Electron Microscopy

ABSTRACT

In this work, an investigation of soot-in-oil samples drawn from the oil sump of a gasoline direct injection (GDI) engine was carried out. Soot particulate was characterised in terms of size, distribution and shape of the agglomerates, and internal structure of the primary particles. The test engine was a 1.6 l modern light-duty EURO IV engine operated at speed between 1600 and 3700 rev/min, and torque between 30 and 120 Nm. After a double oil-flushing procedure the engine was operated for 30 h. Oil samples were drawn from the sump and prepared for Transmission Electron Microscopy (TEM) and High resolution TEM analysis (HRTEM) by a combination of solvent extraction, centrifugation and diethyl ether bathing. Soot agglomerates were measured in terms of their skeleton length and width, and fractal dimension. The mean skeleton length and width were 153 nm and 59 nm respectively. The fractal dimension was calculated using an iterative method and the mean value was found to be 1.44. The primary particles were found to be spherical in shape with some irregularities and presented an average diameter of 36 nm with a mode of 32 nm and standard deviation of 13 nm. The majority of particles showed an inner core and outer shell similar to diesel soot, although an amorphous layer was also clearly visible.

© 2015 The Authors. Published by Elsevier Ltd. This is an open access article under the CC BY license (http://creativecommons.org/licenses/by/4.0/).

## 1. Introduction

Gasoline Direct Injection (GDI) engines are considered an important source of carbonaceous nanoparticles; they produce higher levels of soot as the process of fuel vaporisation and gas-phase mixing remains essentially incomplete [1], even when early fuel injections are used to enable a homogeneous combustion mode [2,3]. This leads to the establishment of sub-stoichiometric mixture-pockets, which are thought to be a significant source of soot formation. Other important mechanisms leading to soot formation have been identified in recent years; primarily, the presence of liquid fuel film over cylinder/piston walls and consequent pool-fire [4,5], as well as the process of direct carbonisation of remaining liquid droplets [6]. The phenomenon of soot formation can be essentially described in terms of three steps: nucleation, growth and oxidation [7]. The process occurs under fuel-rich conditions, in both rich premixed and non-premixed flames, where the local equivalent ratio is more than one. The nucleation process takes place under high temperature conditions, between 1000 and 2800 K, with unburned hydrocarbons, in particular acetylene and polycyclic aromatics hydrocarbons (PAH), being pyrolysed and oxidised. The condensation reactions of these gas-phase species lead to the appearance of a large number of primary soot particles with diameter lower than 2 nm and insignificant soot loading. Surface growth, coagulation and aggregation represent the particles growth. During the surface growth, concentric shells on nuclei and spherules are formed by deposition of hydrocarbon intermediate gas-phase species on particles surface. By means of coagulation the particles collide and merge reducing their number concentration, but keeping the total amount of soot constant. After formation, the collision between particles leads to cluster or chain-like soot aggregates (secondary particles) in which the number of particles decreases with a consequent size increase (PM diameter 100–900 nm). In the overall soot formations process, the precursors, the nuclei and particles can be oxidised if in contact with oxidising species such as $O_2$, O, OH, $CO_2$, and $H_2O$ at the right conditions. Typically, HRTEM shows the primary particles having an outer shell composed of planar shaped crystallites orientated perpendicular to the radius of the particle. The crystallites are comprised of several PAH layers. An inner core, which is constituted by several fine spherules (3–4 nm in diameter) having a nucleus of 1 nm at the central portion, usually characterises primary particles.

The particle number concentration emitted by GDI engines are generally higher than conventional PFI engines and Diesel engines equipped with Particulate Filter (DPF). Most of the soot produced is expelled from the cylinder with the exhaust gases but a small

* Correspondence to: Engine Research Group, Department of Mechanical, Materials and Manufacturing Engineering, The University of Nottingham, University Park, Nottingham NG7 2RD, UK. Tel.: +44 115 95 13815.
*E-mail address:* antonino.larocca@nottingham.ac.uk (A. La Rocca).

http://dx.doi.org/10.1016/j.triboint.2015.01.025
0301-679X/© 2015 The Authors. Published by Elsevier Ltd. This is an open access article under the CC BY license (http://creativecommons.org/licenses/by/4.0/).

proportion is transferred from the cylinder to the lubricating oil. Soot is likely to migrate into the oil film early during the expansion stroke [8]; consequently, the morphology, agglomeration and other characteristics of soot-in-oil are likely to be rather different to exhaust soot. Soot-in-oil has not been subject to oxidation processes to the same extent and hence the outer shell structure is more likely to remain intact. Although only a small proportion of the soot formed in the combustion chamber transfers to the engine oil, it contributes to the lubricant degradation. This is certainly a new challenge for the modern GDI engine as soot-in-oil raises concerns upon wear and engine durability. It is well established that oil thickening has a complex dependence on soot [9]. Various investigators [10,11] have shown that diesel soot build up in oil gives rise to increased engine wear rates; Gautam et al. [12] reported that wear increases with higher soot concentration. Soot reduces the effectiveness of anti-wear additives and its effect on wear depends upon the characteristics of the particles and agglomerates of soot. Abrasive wear occurs and wear scar width closely matches the primary particle size [10]. Oil thickening was found to enhance timing chain elongation due to abrasive action of soot on pins and bushing [13]. Bardasz et al. [14] studied the influence of high number of engine cycles on lubricant oil and that of oil characteristics on engine wear, comparing direct injection and port fuel injection engines and finding increased wear for the first category. There is also a growing interest within the automotive industry to better understand the complex interactions between soot morphology and properties of lubricating oil.

Studies of soot in automotive lubricant oil have mainly focused on particulate matter from diesel engines or carbon black. The percentage by weight of soot in automotive lubricants, assessed using thermo-gravimetric analysis (TGA), was identified as the primary correlation factor affecting oil properties and engine wear [15]. Fourier Transform InfraRed (FTIR) spectroscopy is commonly used to monitor used oil conditions, although this technique is not sufficiently quantitative [9]. Nanoparticle tracking analysis has recently been employed for the measurement of soot agglomerates size distribution and number density from automotive engines oils [16]. Transmission Electron Microscopy (TEM) and High Resolution TEM (HRTEM) are amongst the most widely used techniques available to characterise soot nanoparticles; TEM allows measuring the particle shape and size of projected two-dimensional images of agglomerates as well as the characteristics of individual particles. However, soot-in-oil TEM imaging is more challenging; mineral oil is a contaminant for the electron microscope and leads to instability under the electron beam [17]; very limited information is available in the literature on this topic. Imaging by Cryogenic TEM has also been used by Kawamura et al. [18] and Liu et al. [19] to measure the soot agglomerates size although localised thick layers proved to be challenging and constituted a problem. Li et al. [11] have used solvent extraction technique and ultracentrifugation to prepare the specimen for conventional TEM to analyse soot primary particles from a heavy duty diesel test engine. Clague et al. [7] employed solvent extraction followed by centrifugation to extract soot from used engine oil. A recent study on soot agglomerates shows that centrifugation can alter the distribution of size and shape of these [20]. The solvent dilution technique gives sufficient separation of oil and soot to allow conventional TEM results to be obtained; centrifugation is necessary in the preparation of samples for HRTEM studies of primary particles; these are unchanged by centrifugation. TEM allows measurement of agglomerate size distribution; HRTEM allows examination of the structure and the distribution of the carbon sheets of the primary particles; it provides information about reactivity and nanostructure morphology. The form taken by the soot-in-oil is of interest because of the influence on oil properties, engine performance and wear and for insights into the history of particle formation and growth.

**Table 1**
Typical soot particles dimension from internal combustion engines.

| Reference | Engine type | Soot type | Agglomerate size (nm) | Primary particle size (nm) |
|---|---|---|---|---|
| Bonatesta et al. [35] | GDI | Exhaust | 10–300 | – |
| Uy et al. [33] | GDI | Oil | – | 8–43 |
| Clague et al. [7] | CI | Oil | 150– > 500 | 30–50 |
| La Rocca et al. [20] | CI | Oil | 50–130 | 10–30 |

Engine soot and laboratory flame-generated soot is commonly described in terms of fractal dimension due to the complex morphology [21–25]. Smaller fractal dimensions indicate chain-like structures while larger fractal dimensions indicate clusters. The fractal dimension is a statistical index of complexity and Rogak et al. [26] noted that agglomerate fractal dimensions measured from two-dimensional image projection of three-dimensional structures may be 10–20% lower than geometric dimensions. Given their irregular branched shape, soot particles are also characterised in terms of maximum projected length ($L$) and width ($W$) [26–28]; for chain-like structures, Rogak et al. [29] suggested measuring the skeleton length ($L_{sk}$) of agglomerates.

Barone et al. [30] used TEM to investigate the diameter of aggregate primary particles from GDI exhaust gas soot. They studied particles morphology as a function of injection strategy. Early fuel injections, leading to a more homogeneous air/fuel mixture before combustion, produced nano-particle aggregates ranging between 8 and 52 nm. For retarded fuel injection strategies, most aggregates had fractal-like morphology similar to diesel soot. Mathis et al. [31] studied exhaust soot particles from GDI engines and identified primary particles with a size of about 27 nm. Choi et al. [32] analysed exhaust soot from a GDI engine, showing chain-like structures ranging from 70 to 400 nm in size, with particle cores between 30 and 80 nm. Uy et al. [33] have recently characterised the nanostructure of gasoline soot. They determined and compared the degree of order of the graphitic planes of soot primary particles extracted from the exhaust gas and from engine oil. Soot-in-oil from GDI engine has not been investigated widely; to the authors' best knowledge, its agglomerate size distribution and shape have not been reported in the literature. A summary of the typical dimensions of soot particles from internal combustion engines is reported in Table 1.

The present study is an experimental investigation of soot-in-oil drawn from the oil sump of a modern wall-guided GDI engine. A thorough sample preparation had to be developed to allow for HRTEM imaging of soot-in-oil agglomerates; this is outlined here. Agglomerate and primary particle size distributions are investigated in terms of size, shape and nanostructure. EDX in the TEM allows the elemental components of individual nanoparticles to be investigated. As this technique requires the beam to impinge on the sample for a greater length of time, this technique also benefits from the sample cleaning process developed for HRTEM.

## 2. Experimental setup and sample preparation

### 2.1. Experimental equipment

Engine testing was carried out using a 1.6 l, turbo-charged and intercooled, Euro IV, Direct Injection Spark Ignition, gasoline engine with no modifications, available at Oxford Brookes University. The engine technical specifications are given in Table 2.

The engine was installed on a laboratory test bed and controlled by a Schenck W150 eddy current dynamometer via a CP Engineering CADET engine control and data acquisition system. Fuel consumption was measured via a CP Engineering FMS-400 gravimetric system. The engine was operated for a 30 h time interval at specific steady-state, fully-warm operating conditions crossing a large portion of the part-load running envelope. The delivery of fuel is via a common-rail direct injection system; injection pressure is regulated via the ECU as a function of load and speed, with a maximum value of 120 bar. The fuel used for testing was pump-grade, unleaded gasoline with the following average specifications:

RON=95
MON=85
Stoichiometric AFR=14.4
Nominal latent heat of vaporisation=0.34 MJ/kg
Max sulphur content=50 ppm
Max aromatics content=35% (by volume)
Max renewable content=4.5% (by volume)

### 2.2. Soot-in-oil sampling

At the beginning of the testing period the engine was flushed twice with clean oil; a further final oil change followed. Each flushing included a full oil and filter change, as well as running the engine for 3 h in fully warm and steady state operating condition at a speed of 1600 rev/min and at a brake load of 15 Nm. The double flush-and-drain procedure was sufficient to obtain drained oil visibly not dissimilar to new oil. Similarly, Arcoumanis et al. [34] employed two equal consecutive flushing procedures to remove most used oil and residue from the engine. The characteristics of soot nanoparticles in engine oil were studied by sampling the lubricating oil at the end of 30 h of operation. Although the mix of operating conditions covered was defined for other purposes, this was sufficiently varied to suggest the range of agglomerates formed would be representative of urban environment use. At the end of the testing, oil samples were drawn from the sump for the investigation of the soot content.

### 2.3. Soot-in-oil measurements

Soot-in-oil characterisation was performed at the Soot Diagnostics Suite at the University of Nottingham. As suggested by La Rocca et al. [20], samples of soot extracted from engine oil were prepared using a solvent extraction process, diluting the oil at a dilution ratio of 1:60 in heptane. This produces a heptane solution containing a much lower oil content, and also at a suitable low viscosity to allow deposition onto TEM grids. Following deposition, the solvent evaporates rapidly to leave soot particles of varying sizes and aggregations. This process puts little strain on the soot aggregates and it is expected to reveal a structure typical of the soot as it was in the engine oil. Samples were then subjected to close-to-vacuum conditions in order to enhance the evaporation of the solvent. Level of contamination was still considerably high, and its progressive build-up on the sample under the electron beam led to sample becoming gradually darker forming distinctive dark rings as depicted in Fig. 1, which prevented imaging and rendered the samples unsuitable for further analysis.

**Table 2**
Test engine technical specifications.

| | |
|---|---|
| Displacement (cc) | 1598 |
| Stroke (mm) | 77 |
| Compression ratio | 10.5:1 |
| Connecting rod length (mm) | 138.4 |
| Combustion chamber | 4-Valve, central spark plug, pent-roof design |
| Engine type | In-line 4-cylinder |
| Cycle | 4-stroke spark ignition |
| Fuel injection system | Direct injection common rail |
| Fuel injectors | Side-mounted, wall-guided spray |
| Maximum injection pressure (bar) | 120 |
| Maximum engine speed (rev/min) | 6000 |
| Maximum rated torque (Nm) | 240 |

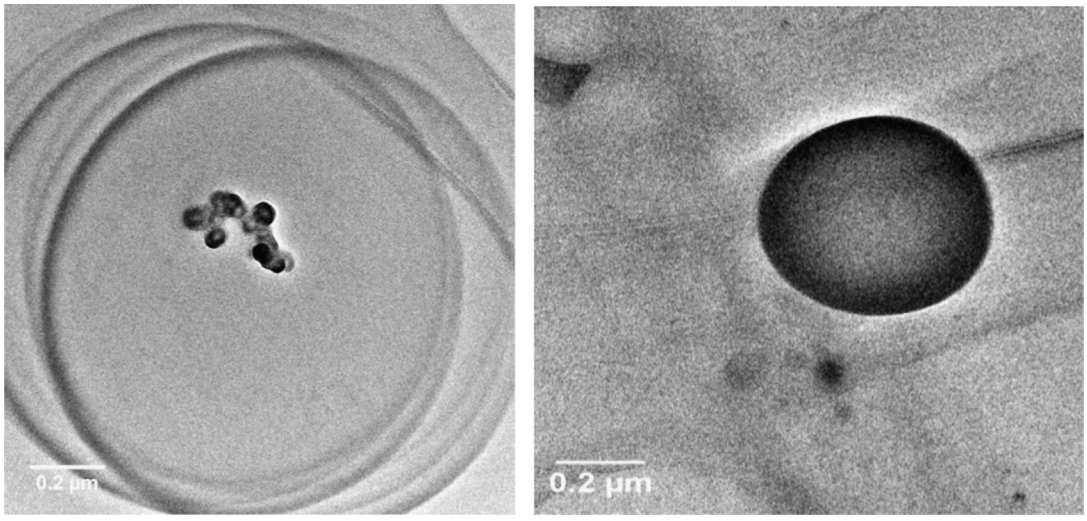


**Fig. 1.** TEM image showing effects of contamination and the characteristic dark rings formed at the edge of the area exposed to the electron beam.

Two stages of diethyl bathing were employed to reduce contamination and allow for agglomerate size measurements. For HRTEM analysis, centrifugation was performed on the diluted oil/heptane solution following the work of La Rocca et al. [20]. The number of centrifugation stages at 14,000 rev/min and 25 °C for 90 min was increased to six in the present study. After each stage, the liquid phase was replaced with equal amount of pure heptane. Samples were also subjected to 30 min of ultrasonic bathing. 3 μl of the soot suspension in heptane were dispersed onto TEM support films and subsequently washed with diethyl ether.

## 3. Results and discussion

Fig. 2 shows typical TEM images of agglomerates after solvent extraction. Several 1–2 nm particles were found on the grid. Similar particles were found in diesel soot-in-oil samples in [20] and were considered to be oil additives.

In this work, soot-in-oil particles were measured in terms of their skeleton length, $L_{sk}$, and width, $W_{sk}$, and fractal dimension. $L_{sk}$ and $W_{sk}$ were inferred from 2-D TEM images using an open architecture image processing software, ImageJ, whilst a MATLAB algorithm was created specifically for calculating the fractal dimension. The algorithm followed the iterative method proposed in [21], which is not discussed in details here for brevity. Soot agglomerates were measured based on the skeleton criterium, as this results in a better representation of the aspect ratio [20]. Fig. 3(a) and (b) illustrates the skeleton length and width frequency distribution of the agglomerates. The mean skeleton length, $L_{Sk}$ and width, $W_{Sk}$ were found to be 153 nm and 59 nm, respectively. 66% of the agglomerates presented a skeleton length between 90 nm and 180 nm, with $L_{Sk}$ ranging from 53 nm to 405 nm. Long agglomerates with skeleton lengths longer than 300 nm accounted for 9% of the agglomerates. The skeleton width spanned from 33 nm to 102 nm, with 70% of agglomerates in the range 60–80 nm.

GDI soot agglomerate size was found to be comparable to diesel engine soot-in-oil as reported in literature. Soot-in-oil agglomerates drawn from diesel engines show a modest branched morphology, and exist in clusters and chain-like structures with average hydraulic diameter of 100 nm [16]. Similar agglomerates were found by Clague et al. [7] in a study in which soot was compared to black carbon. Diesel soot investigated by La Rocca et al. [20] had an average skeleton length of 131.8 nm measured from TEM projections and were composed of spherical primary particles of 12–40 nm.

In this work, particles with an aspect ratio $L_{Sk}/W_{Sk} < 2.5$ are considered to be clusters and particles with an $L_{Sk}/W_{Sk}$ ratio $> 2.5$ to be chains. The present investigation of GDI soot nanoparticles found 53.6% of the agglomerates analysed as clusters with very modest branching, whilst 46.4% were chain-like structures. Typical agglomerates found in such samples are shown in Fig. 2. A similar measurement was carried out in [20], where a slight majority agglomerates was present as chain-like structures; in that investigation, 46% of the agglomerates showed an aspect ratio $< 2.5$ and 54% showed an aspect ratio $> 2.5$.

Fig. 3(d) shows the fractal dimension frequency distribution of the soot agglomerates analysed in the present study. As shown, 97% of the measured $D_f$ varied in the range 1.1–1.8; similar fractal dimensions, comprised between 1.2 and 1.74, have been reported by Li et al. [11] in a study on in-cylinder diesel soot. The measured fractal dimension indicates the presence of a majority of short-

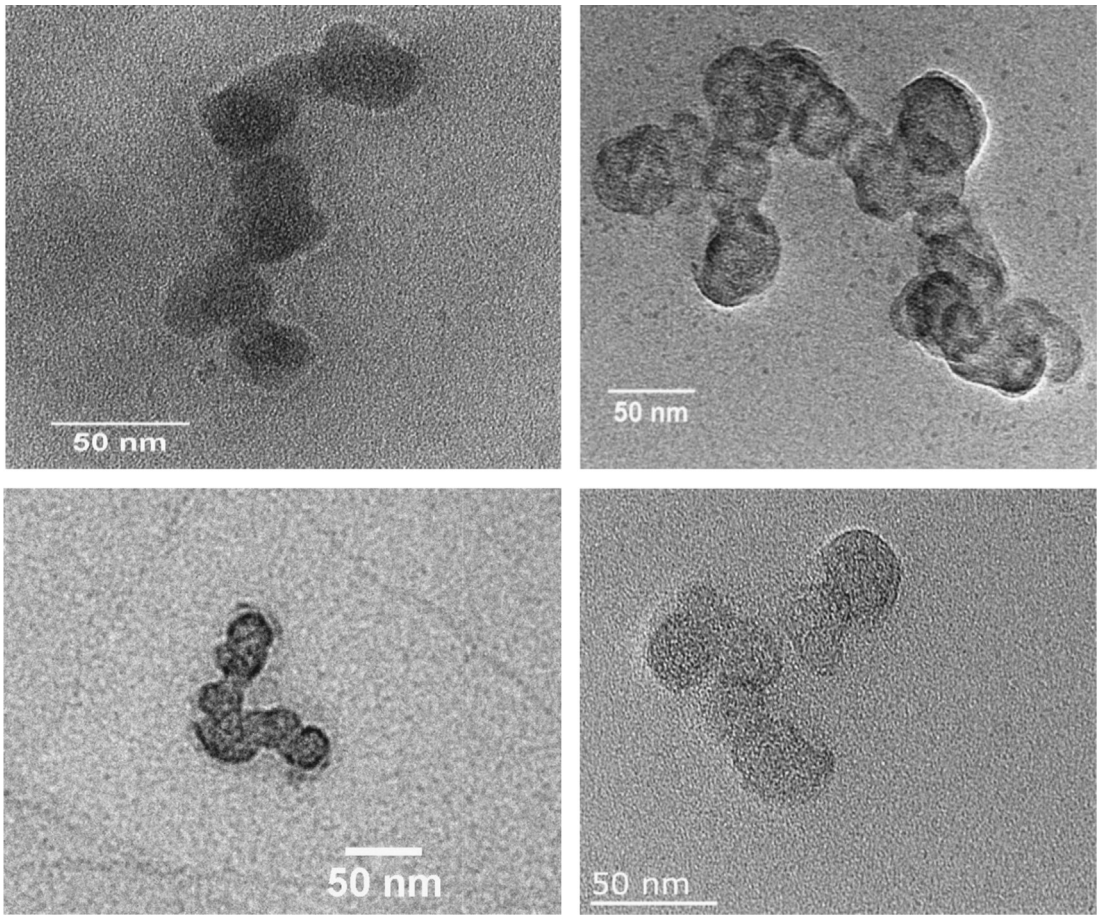


**Fig. 2.** Agglomerates images (TEM) from soot-in-oil samples prepared by solvent extraction.

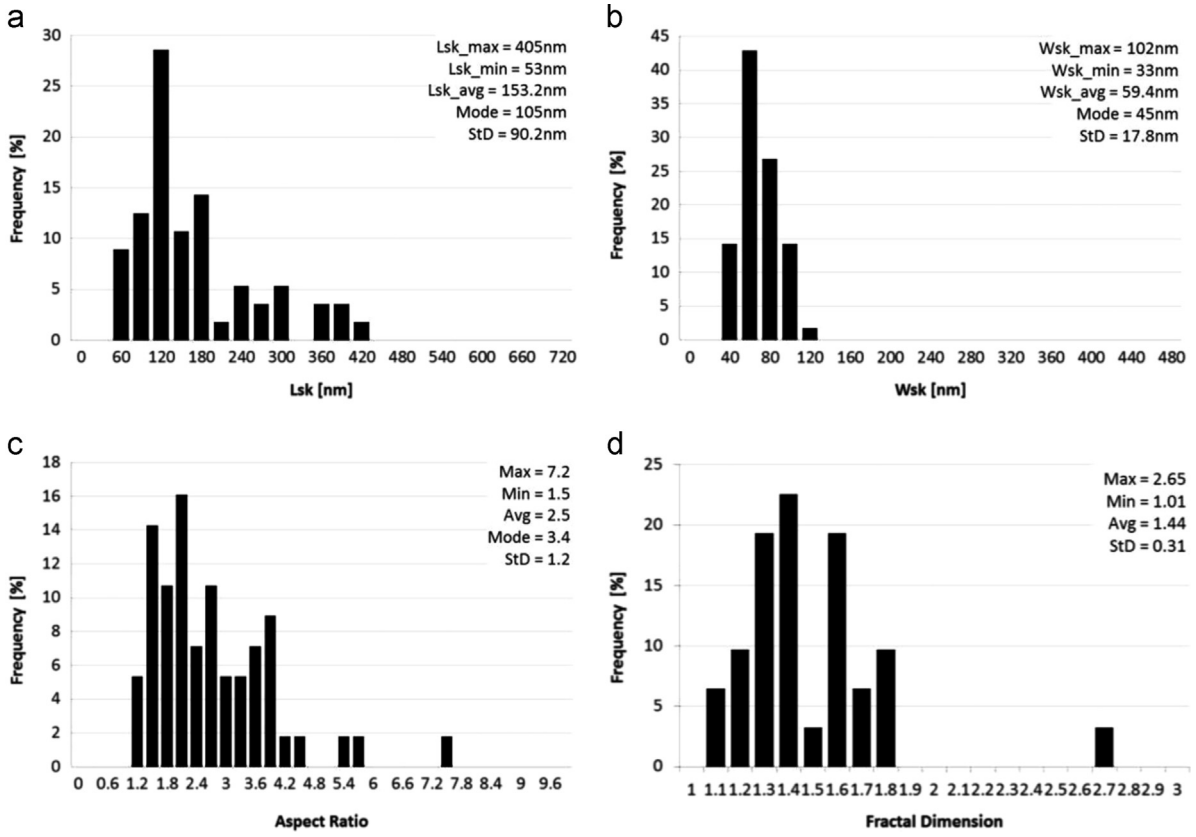


**Fig. 3.** Frequency distribution of soot-in-oil samples prepared by solvent extraction: (a) agglomerate skeleton length, (b) skeleton width, (c) aspect ratio and (d) fractal dimension.

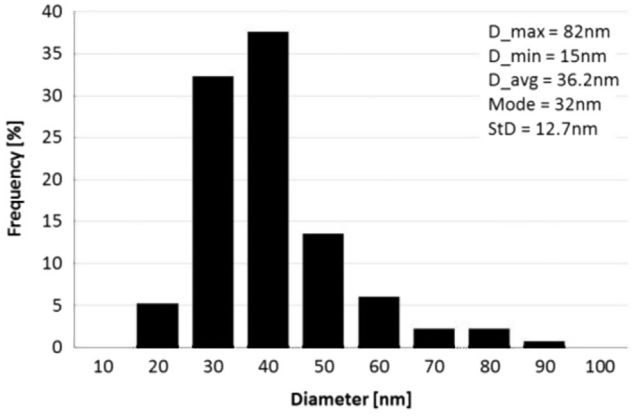


**Fig. 4.** GDI soot primary particles diameter distribution of soot-in-oil samples.

branched structures. The soot agglomerates analysed in this investigation were not dissimilar to typical agglomerates from diesel engines used oils. Differences in agglomerate sizes could be associated with differences in engine operating conditions, fuel type and details of engine features such as fuel injector. Observations on how engine conditions affect agglomerate size can be found in a sister publication by the authors [35]. In that study, experimental measurements of agglomerate soot size distribution have been taken from the same engine, covering a large portion of the part-load running envelope at different engine speed and load.

HRTEM samples were prepared for analysis as discussed in the methodology section; primary particles size distribution and their internal structure were of interest. Fig. 4 shows the diameter frequency distribution of oil soot primary particles. Soot-in-oil primary particles presented a mean diameter of 36.2 nm with a mode of 32 nm and standard deviation of 12.7 nm. Primary particles diameters spanned from 20 nm to 90 nm, with 88.7% of the particles in the range 20–50 nm, 11.3% equal or larger than 60 nm.

Diesel soot-in-oil primary particles have been reported to be in the range 10 nm to 35 nm, with a mean diameter of 20.2 nm [20]. In a separate investigation, Su et al. [36] analysed the microstructure of diesel soot-in-oil primary particles from a Euro IV engine, and found that the primary particle diameter is significantly smaller compared to a conventional diesel engine, specifically in the range 3–15 nm. This was attributed to the higher oxidation rates and their operation at higher pressures and temperature. Primary particles analysed in the present work are found to be larger in sizes compared to size distributions from DI diesel engines [17]. As reported by Bonatesta et al. [35], and in line with the relevant literature [31,37,38], the vast majority of exhaust soot emitted by the wall-guided GDI test engine can be considered as primary particles in the 10 to 100 nm diameter range, whereas in excess of 55% is emitted in nucleation mode (below 50 nm).

Analysis of soot-in-oil samples allows characterisation of the nanostructure of the primary particles as it was at the time it transferred into the lubricating oil from the combustion chamber. In the soot-in-oil primary particles pictured in Figs. 5 and 6, a core–shell structure similar to that found in diesel particles can be observed. Interestingly, the vast majority of primary particles analysed in this work presented a core-shell structure, along with an unusual amorphous layer covering the particle. This was not observed in other studies of diesel soot particulate reported in the literature. Minimising beam exposure prior to imaging did not result in any significant apparent change in the thickness of this

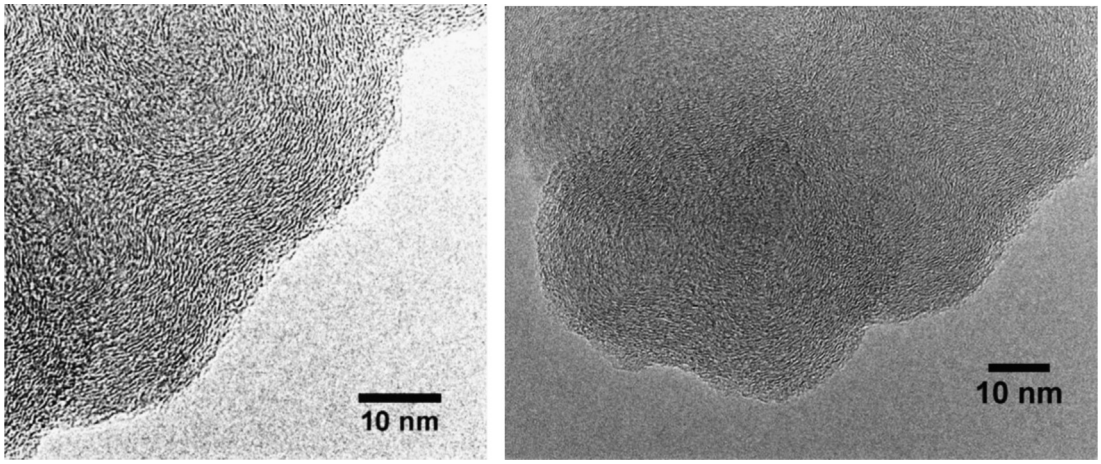


**Fig. 5.** GDI soot-in-oil TEM image showing internal structure of primary particles (Image on the left has contrast enhanced using ImageJ to improve the fringes visibility).

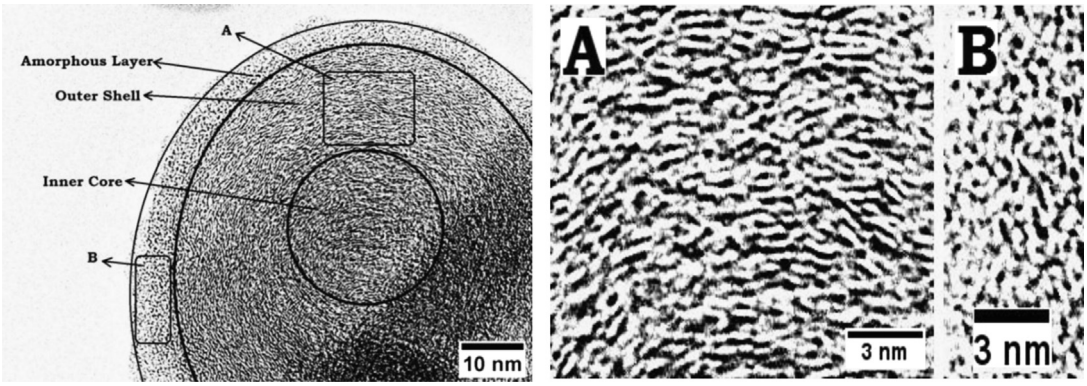


**Fig. 6.** Core–shell structure of GDI soot-in-oil primary particles showing central core 25 nm in diameter, shell 16 nm thick and amorphous layer 5 nm thick. A and B show details with contrast enhanced using ImageJ to improve the fringes visibility.

layer, although long beam exposure times have been observed to produce a variable amount of additional amorphous carbon.

Primary particle nanostructure details are given in Fig. 6A and B; both detailed images were adjusted in terms of brightness and contrast in order to improve the visualisation of the structure. Soot primary particles show a turbostratic structure, similar to diesel soot samples [20], with characteristic core and shell. Two layers are clearly distinguishable in the shell. The inner layer is of typical graphitic nature. The inner core is 25 nm in diameter while the outer shell measured 16–20 nm in thickness; this was composed of lamellae ordered in an onion-like structure around the inner core, similar to the structures reported in [20] and [24], and covered by a layer of amorphous carbon. The outer shell is significantly thicker than the one observed in Fig. 5, which shows a bucky-onion structure of 8–12 nm. The latter being typical of diesel particles as reported in [20].

Soot reactivity is essentially dictated by the outer shell structure. Although the classic core-shell structure is clearly visible in all particles, the wider graphitic layers concentrically orientated, and typically with fewer reactive sites [39], are covered by an amorphous 5 nm layer with very short segments. This leads to an increase of edge sites and consequently to an increase of overall reactivity as reported by Vander Wal [40]. Uy et al. [33] also reported gasoline soot primary particles being of amorphous structure.

Another interesting feature of the GDI soot particles is the recurrent presence of crystalline structures on the primary particle surface, as depicted in Fig. 7. Prolonged exposure to the electron beam at normal imaging intensities frequently led to decomposition, suggesting many of these are volatile structures. This was also observed by Uy et al. [33]. In Fig. 7a, the spacing between the layers of the particle is about 1 Å, strongly suggesting graphitic nature. Kubicki [41] points out that lamellar graphitic structures are possible and can be formed from the gas phase. This may be more applicable to gasoline derived soot where the hydrocarbons involved are more volatile compared to diesel [36]. Fig. 7b shows a darker particle on the bottom right of the carbon material; being significantly darker despite being much smaller indicates it is a heavier material than the mostly carbon soot particle.

Non carbon structures were separately identified using High Angle Annular Dark Field – Scanning TEM (HAADF-STEM); the EDX spectra were obtained from a range of these structures found on the grid. Table 3 shows a selection of the spectra, illustrating the elements most frequently found.

More generally, TEM-EDX analysis of non-soot nanoparticles in the sample showed the widespread presence of O, consistent with most of these materials being heavily oxidised. P, S, Ca, Zn, Mg, Mo and Na have previously been listed as coming from engine oil additives [33]. All these elements have been observed in this analysis, with S, Ca and Mg observed widely. Similarly, Fe, Cr, Al and Cu were identified as coming from wear metals. Particles with Al and Fe content were identified in this work, Cu could not be identified using EDX-TEM due to the use of Cu TEM grids.

## 4. Conclusions

Soot agglomerates extracted from engine oil from a modern gasoline direct injection engine have been characterised for the first time, with the aim of assessing size, distribution and shape.

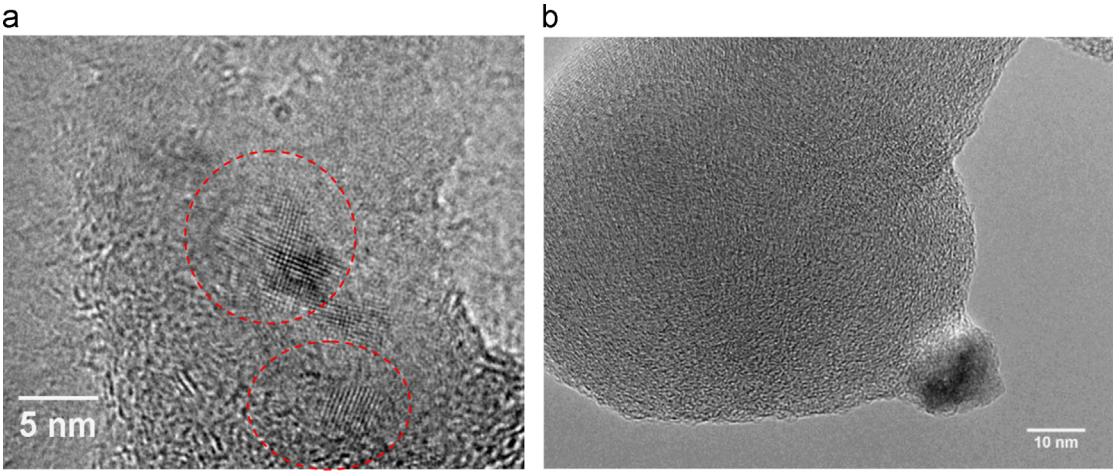


**Fig. 7.** HRTEM images revealing crystalline structures deposited on soot-in-oil particles.

**Table 3**
EDX spectra from four non-carbon structures found on the grid. The C and O percentages include the contribution from the support film.

| Element | Particle 1 (wt%) | Particle 2 (wt%) | Particle 3 (wt%) | Particle 4 (wt%) |
|---|---|---|---|---|
| **Al** | 0 | 0 | 19.03 | 0 |
| **C** | 71.58 | 53.52 | 42.37 | 50.61 |
| **Ca** | 2.55 | 3.39 | 1.74 | 0 |
| **Fe** | 0 | 0 | 0 | 13.56 |
| **K** | 0 | 4.16 | 0 | 0 |
| **Mg** | 1.67 | 1.71 | 1.74 | 1.33 |
| **Mo** | 4.05 | 0 | 0 | 0 |
| **Na** | 0 | 3.7 | 0 | 0 |
| **O** | 14.62 | 26.8 | 27.26 | 34.5 |
| **P** | 0 | 4.21 | 0 | 0 |
| **S** | 0.71 | 2.51 | 1.32 | 0 |
| **Si** | 4.79 | 0 | 2.08 | 0 |
| **Ti** | 0 | 0 | 4.44 | 0 |

The nanostructure of the primary particles was also investigated. A robust methodology to produce samples for TEM and HRTEM was developed and outlined.

Agglomerate size was given in terms of skeleton length, width and fractal dimension. At the macro scale, the GDI soot agglomerates are remarkably similar to agglomerates from light duty diesel engines as reported in the literature. The mean length and width were found to be 153 nm and 59 nm. 54% of the agglomerates presented an aspect ratio $< 2.5$, indicating a small predominance of compact structures with very modest branching. The mean fractal dimension of the agglomerates was calculated to be 1.44.

Conversely, the primary particles differ in nanostructure from a typical diesel soot particle. GDI primary particles are spherical in shape, with some irregularities. The mean diameter was found to be 36 nm. An inner core and outer shell structure was found in the majority of the particles. The wider graphitic layers concentrically orientated, and typically with fewer reactive sites, were covered by an amorphous 5 nm layer with very short segments.

Volatile lamellar graphitic structures were found deposited on the external surface of soot-in-oil primary particles. TEM-EDX analysis of non-soot nanoparticles in the sample showed the widespread presence oil additive elements and wear metals.

## References

[1] Piock W, Hoffmann G, Berndorfer A, Salemi P, Fusshoeller B. Strategies towards meeting future particulate matter emission requirements in homogeneous gasoline direct injection engines. SAE Int J Engines 2011;4(1):1455–68.

[2] Peckham MS, Finch A, Campbell B, Price P, Davies MT Study of particle number emissions from a turbocharged gasoline direct injection (GDI) engine including data from a fast-response particle size spectrometer, SAE technical paper 2011-01-1224; 2011. http://dx.doi.org/10.4271/2011-01-1224.

[3] Williams B, Ewart P, Wang X, Stone R, Ma H, Walmsley H, et al. Quantitative planar laser-induced fluorescence imaging of multi-component fuel/air mixing in a firing gasoline-direct-injection engine: effects of residual exhaust gas on quantitative PLIF. Combust Flame 2010;157(10):1866–78.

[4] Velji A, Yeom K, Wagner U, Spicher U et al. Investigations of the formation and oxidation of soot inside a direct injection spark ignition engine using advanced laser-techniques, SAE technical paper 2010–01-0352; 2010.

[5] Lucchini T, D'Errico G, Onorati A, Bonandrini G, Venturoli L, Di Gioia R. Development and application of a computational fluid dynamics methodology to predict fuel–air mixing and sources of soot formation in gasoline direct injection engines. Int J Engine Res 2014;15(5):581–96.

[6] Maricq MM, Podsiadlik DH, Brehob DD, Haghgooie M Particulate emissions from a direct-injection spark-ignition (DISI) engine, SAE technical paper 1999–01-1530; 1999.

[7] Clague ADH, Donnet JB, Wang TK, Peng JCM. A comparison of diesel engine soot with carbon black. Carbon 1999;37(10):1553–65.

[8] Wan Mahmood W, La Rocca A, Shayler P, Bonatesta F et al. Predicted paths of soot particles in the cylinders of a direct injection diesel engine, SAE technical paper 2012-01-0148; 2012. http://dx.doi.org/10.4271/2012-01-0148.

[9] Asango A, La Rocca A, Shayler P Investigating the effect of carbon nanoparticles on the viscosity of lubricant oil from light duty automotive diesel engines, SAE technical paper 2014-01-1481; 2014. http://dx.doi.org/10.4271/2014-01-1481.

[10] Green DA, Lewis R. The effects of soot-contaminated engine oil on wear and friction: a review. Proc Inst Mech Eng Part D J Automob Eng 2008;222(9):1669–89.

[11] Li S, Csontos A, Gable B, Passut C, Jao T Wear in cummins M-11/EGR test engines, SAE technical paper; 2002-01-1672; 2002. http://dx.doi.org/10.4271/2002-01-1672.

[12] Gautam M, Chitoora K, Durbhaa M, Summers JC. Effect of diesel soot contaminated oil on engine wear investigation of novel oil formulations. Tribol Int 1999;32:687–99.

[13] Polat O, Ebrinc A, Ozen C, Akca S Timing chain wear assessment with different type of oils, SAE technical paper 2009-01-0198; 2009. http://dx.doi.org/10.4271/2009-01-0198.

[14] Bardasz E.A., Arters D.C., Schiferl E.A., Righi D.W. A comparison of gasoline direct injection and port fuel injection vehicles: Part II – lubricant oil performance and engine wear, SAE technical paper 1999-01-1499; 1999. http://dx.doi.org/10.4271/1999-01-1499.

[15] La Rocca A, Di Liberto G, Shayler P, Parmenter C, et al. A novel diagnostics tool for measuring soot agglomerates size distribution in used automotive lubricant oils. SAE Int J Fuels Lubr 2014;7(1):301–6.

[16] La Rocca A, Di Liberto G, Shayler PJ, Fay MW, Parmenter CDJ. Application of nanoparticle tracking analysis platform for the measurement of soot-in-oil agglomerates from automotive engines. Tribol Int 2014;70:142–7.

[17] Shuff PJ, Clarke LJ. Imaging of lubricating oil insolubles by electron microscopy. Tribol Int 1991;24(6):381–7.

[18] Kawamura M, Ishiguro T, Fujita K, Moromoto H. Deterioration of antiwear properties of diesel engine oils during use. Wear 1998;123:269–80.

[19] Liu C, Nemoto S, Ogano S. Effect of soot properties in diesel engine oils on frictional characteristics. Tribol Trans 2003;46(1):12–8.

[20] La Rocca A, Di Liberto G, Shayler PJ, Fay MW. The nanostructure of soot-in-oil particles and agglomerates from an automotive diesel engine. Tribol Int 2013;61:80–7.

[21] Lee KO, Cole R, Sekar R, Choi MY, Kang JS, Bae CS, et al. Morphological investigation of the microstructure, dimensions, and fractal geometry of diesel particulates. Proc Combust Inst 2002;29(1):647–53.
[22] Zhu J, Lee KO, Yozgatligil A, Choi MY. Effects of engine operating conditions on morphology, microstructure, and fractal geometry of light-duty diesel engine particulates. Proc. Combust Inst 2005;30(2):2781–9.
[23] Neer A, Koylu UO. Effect of operating conditions on the size, morphology, and concentration of submicrometer particulates emitted from a diesel engine. Combust Flame 2006;146(1–2):142–54.
[24] Lapuerta M, Ballesteros R, Martos FJ. The effect of diesel engine conditions on the size and morphology of soot particles. Int J Veh Des 2009;50(1):91–106.
[25] Annele K, Virtanen K, Ristimäki JM, Vaaraslahti KM, Keskinen J. Effect of engine load on diesel soot particles. Environ Sci Technol 2004;38(9):2551–6.
[26] Rogak SN, Flagan RC. Characterization of the structure of agglomerate particles. Part. Part. Syst. Charact. 1992;9:19–27.
[27] Samson RJ, Mulholland GW, Gentry JW. Structural analysis of soot agglomerates. Langmuir 1987;3(2):272–81.
[28] Park A, Kittelson DB, Zachariah MR, McMurry JC. Measurement of inherent material density of nanoparticle agglomerates. J Nanopart Res 2004;6:267–72.
[29] Rogak SN, Flagan RC, Nguyen HV. The mobility and structure of aerosol agglomerates aerosol. Sci Technol 1993;18(1):25–47.
[30] Barone TL, Storey JME, Youngquist AD, Szybist JP. An analysis of direct injection spark-ignition (DISI) soot morphology. Atmos Environ 2012;49:268–74.
[31] Mathis U, Kaegi R, Mohr M, Zenobi R. TEM analysis of volatile nanoparticles from particle trap equipped diesel and direct-injection spark-ignition vehicles. Atmos Environ 2004;38:4347–55.
[32] Choi K, Kim J, Myung CL, Lee M, Kwon S, Lee Y, et al. Effect of the mixture preparation on the nanoparticle characteristics of gasoline direct-injection vehicles. J Automob Eng: Part D 2012;226(11):1514–24.
[33] Uy D, Ford MA, Jayne DT, O'Neill AE, Haack LP, Hangas J, et al. Characterization of gasoline soot and comparison to diesel soot: morphology, chemistry, and wear. Tribol Int 2014;80:198–209.
[34] Arcoumanis C., Duszynski M., Lindenkamp H., Preston H. Measurements of the lubricant film thickness in the cylinder of a firing diesel engine using LIF, SAE technical paper 982435; 1998. http://dx.doi.org/10.4271/982435.
[35] Bonatesta F, Chiappetta E, La Rocca A. Part-load particulate matter from a GDI engine and the connection with combustion characteristics. Appl Energy 2014;124:366–76.
[36] Su DS, Jentoft DE, Muller JO, Jacob E, Simpson CD, Tomovic Z, et al. Microstructure and oxidation behaviour of Euro IV diesel engine soot: a comparative study with synthetic model soot substances. Catal Today 2004;90:127–32.
[37] Braisher M., Stone R., Price P. Particle number emissions from a range of European vehicles, SAE technical paper, 2010-01-0786; 2010. http://dx.doi.org/10.4271/2010-01-0786.
[38] Price P., Stone R., Collier T., Davies M. Particulate matter and hydrocarbon emissions measurements: comparing first and second generation DISI with PFI in single cylinder optical engines, SAE technical paper, 2006-01-1263; 2006. http://dx.doi.org/10.4271/2006-01-1263.
[39] Donnet JB. Structure and reactivity of carbons: from carbon black to carbon composites. Carbon 1982;20(4):267–82.
[40] Vander Wal RL, Tomasek AJ. Soot oxidation: dependence upon initial nanostructure. Combust Flame 2003;134(1–2):1–9.
[41] Kubicki JD. Molecular mechanics and quantum mechanical modeling of hexane soot structure and interactions with pyrene. Geochem Trans. 2000;1:41–6. http://dx.doi.org/10.1039/b004601i.